THE ASTROPHYSICAL JOURNAL, 448:548–562, 1995 August 1

COLLISIONS OF ELLIPTICALS AND THE ONSET OF FANAROFF-RILEY TYPE I RADIO SOURCES

LUIS COLINA[1]
Space Telescope Science Institute, 3700 San Martin Drive, Baltimore, MD21218
AND
LOURDES DE JUAN
Departamento de Física Teórica, Módulo C-XI, Universidad Autónoma de Madrid, Cantoblanco, 28049 Madrid, Spain
Received 1994 October 11; accepted 1995 February 13

ABSTRACT

This paper presents the first detailed quantitative study on the morphological characterization of Fanaroff-Riley type I radio source (FR I) host galaxies. The study is based on a two-dimensional isophote analysis of the largest sample (44) available so far of FR I host galaxies.

FR I host galaxies are luminous ellipticals following the same $\mu_e - r_e$ relation as nonradio ellipticals. However, a large fraction (60%) of FR I host galaxies in the sample show at least two of the following morphological peculiarities: (1) isophote twists which are larger than 15°, (2) isophote displacements which are larger than 3.5%, (3) excesses over a de Vaucouleurs law which exceeds 0.10 mag arcsec^{-2} at radii beyond r_e, and (4) one companion galaxy at a distance of less than 50 kpc.

These morphological peculiarities are the signature of a recent strong gravitational collision. The collision, involving a pair of ellipticals, is characterized by (1) a median mass ratio (companion to FR I host galaxy) of $\sim$0.2, (2) a median projected distance of $\sim$23 kpc, (3) a median relative velocity of $\sim$492 km s^{-1}, (4) a median age of $\sim 4.0 \times 10^7$ years, and (5) a median interaction strength parameter of 0.19.

Collisions between ellipticals which share the above mentioned mean properties appear to be very efficient in generating a FR I radio source. Therefore, the scenario of the onset of an active nucleus by galaxy collisions, well established for very luminous starbursts and radio galaxies, can also be extended to FR I radio sources. In a broader scenario, the conclusions of this paper also reinforce the idea that collisions between different type of galaxies give rise to different type of activity in their nuclei: collisions involving two spirals produce luminous circumnuclear starbursts, collisions involving one elliptical and one spiral generate powerful Fanaroff-Riley type II sources (FR II), which collisions between twoellipticals ignite FR I radio sources.

Subject headings: galaxies: active — galaxies: elliptical and lenticular, cD — galaxies: interactions — galaxies: photometry — radio continuum: galaxies

1. INTRODUCTION

Observational evidence collected over the past few years has led to the generally accepted consensus that collisions and mergers of gas-rich systems are very efficient in generating and maintaining starburst and nonthermal activity in the nuclei of galaxies. High-luminosity and ultraluminous *IRAS* galaxies show that extensive circumnuclear star-formation is generated during collision and merging involving gas-rich spiral galaxies (Sanders et al. 1988; Melnick & Mirabel 1990). Powerful FR II radio sources are located in luminous ellipticals showing morphological characteristics of a past collision/merger with a gas-rich spiral (Heckman et al. 1986), while quasars show a disrupted morphology and close companions (Hutchings & Neff 1992).

The evidence for the onset of a Seyfert type or low-luminosity FR I radio source by galaxy collisions is less compelling (see review by Heckman 1991, and references therein). However, based on qualitative morphological arguments drawn from a large sample of mostly low-luminosity radio galaxies (FR I, i.e., $\log P_{1.4\,\mathrm{GHz}} \leq 25$ W Hz^{-1}), Colina and Pérez-Fournon argued that low luminosity radio sources could be generated by the collision of two ellipticals (Colina & Pérez-Fournon 1990a, b). This suggestion was confirmed by an independent study of FR I host galaxies from the Bologna catalog of radio sources, where up to 75% of the galaxies show morphological peculiarities indicating a gravitational interaction with a close companion galaxy (González-Serrano, Carballo, & Pérez-Fournon 1993). Also, detailed models of the collision of NGC 4782/4783 and its effect on the radio morphology of the associated radio source 3C 278 (Borne & Colina 1993) supports the collisionally induced nonthermal activity scenario in low-luminosity FR I radio galaxies.

In this paper we present for the first time a detailed quantitative study of the largest sample of FR I host galaxies for which a detailed isophotal analysis is available (González-Serrano et al. 1993; de Juan, Colina, & Pérez-Fournon 1994). Section 2 summarizes the basic properties of the sample. Section 3 shows the empirical evidence in favor of collision between galaxies and illustrate how the gravitational interaction is parameterized as a function of the following elements: isophote twist, appearance of nonconcentric isophotes, departures from a de Vaucouleurs law, and presence of nearby companions. Section 4 is dedicated to the physical characterization of the collision in terms of the type of galaxies involved in the collision, the values for the pair mass ratio, the projected distance, the relative velocity, the time elapsed since the closest encounter, and the strength of the gravitational interaction. Finally, § 5 presents the results within a more general scenario

[1] On assignment from the Space Science Department of ESA.

of nuclear/circumnuclear activity induced by collision of galaxies and in which different kinds of activity are generated by collisions between different types of host galaxies.

2. THE SAMPLE

The galaxy sample consist of 44 low-redshift ($z \leq 0.10$) galaxies associated with low luminosity ($\log P_{1.4\,\mathrm{GHz}} \leq 25.1$ W Hz^{-1}) radio sources showing a double-sided radio jet morphology, i.e., Fanaroff-Riley type I radio sources. The average luminosity in the sample is $\log P_{1.4\,\mathrm{GHz}} = 24.3 \pm 0.6$ W Hz^{-1}. For all galaxies in this sample, broadband CCD photometry and a two-dimensional isophote analysis are available. Note that the optical counterpart of 3C 75 consists of a dumbbell system where the two galaxies have associated radio sources. In the rest of the paper 3C 75 will be considered as two independent sources.

The first subsample of 25 galaxies consist of galaxies from the sample of Colina & Pérez-Fournon (1990a, b). These galaxies were selected from the list of well defined radio jet sources given by Bridle & Perley (1984). Details on the two-dimensional isophote analysis for this subsample can be found in de Juan et al. (1994).

The second subsample of 19 galaxies was obtained from a study of FR I sources selected from the Bologna catalog of radio sources. Details of the sample and of the isophote analysis for this subsample can be found in González-Serrano et al. (1993). Complementary two-dimensional isophotal analysis has been done by us for a few galaxies for which detailed information on the companion galaxy was not available.

Table 1 list some basic properties, including cluster membership, for the galaxies in the sample. Specific comments on each of the galaxies can be found in the references listed above. Throughout the paper, effective magnitudes are given in the r filter of the Gunn-Thuan system. Galaxies for which the original values are given in Johnson V-magnitudes, have been transformed to the r Gunn-Thuan system using the Kent (1985) set of Johnson to Gunn-Thuan system transformations. A Hubble constant of $H_0 = 75$ km s^{-1} Mpc^{-1} is adopted throughout the paper.

3. FR I HOST GALAXIES: SIGNATURES OF COLLIDING GALAXIES

The isophotal analysis of the FR I host galaxies in the sample indicates that a large fraction of the sample shows signatures of gravitational interaction. These signatures include isophote twisting, nonconcentric isophotes, light profile excess above a $r^{1/4}$ law, or the presence of a close companion with signs of a disrupted morphology. In this section characteristic values for these morphological distortions are evaluated and compared to other samples of nonradio ellipticals. This comparison reveals that isophotal distortions are very frequent and quantitatively more important for FR I host galaxies than for nonradio ellipticals. Projected pairs, i.e., normal ellipticals seen in projection but not gravitationally interacting, could mimic the type of peculiar morphological characteristics mentioned above. Several tests were done with the interactive two-dimensional isophotal analysis to recover the parameters of simulated projected pairs. The outputs of the tests always give the expected answers to within the uncertainties generated by the algorithm (see de Juan et al. 1994 for details).

3.1. *Isophote Twists*

Isophote twists are indicated by the change in the position angle of the major axis of the stellar component as a function of radius. Two different measures of the isophote twists in the FR I host galaxies of the present sample are given in Table 2. The first measurement indicates the maximum twist found in each galaxy per decade in isophotal radius (column labeled "grad PA" in Table 2), while the second measurement represents the maximum absolute twist over the whole range of isophotal radius (column labeled as ΔPA in Table 2).

It is known that due to triaxiality, rounder isophotes tend to show some isophote twist. Typical twists due to this effect correspond, on average, to about 5°–10° for samples of normal ellipticals (Benacchio & Galletta 1980; Bender, Döbereiner, & Möllenhoff 1988; Sparks et al. 1991). In these samples, only a small fraction of the galaxies (~10%) shows twists larger than 15°.

Histograms in Figure 1 represent the distributions of position angle gradient (grad PA) and absolute twist (ΔPA) for the FR I host galaxies and for the sample of nonradio ellipticals from Sparks et al. (1991). Both kind of histograms show clear differences for each sample. First, the average values of ΔPA for both samples are 30° and 10° (median values 14° and 4°), respectively, indicating that isophote twists in FR I host galaxies are very much larger than in nonradio ellipticals. Second, FR I host galaxies spread over a wider range of values, with 47% of the galaxies showing twists larger than 15°, while this fraction corresponds to only 13% for Sparks nonradio ellipticals. Average values of grad PA are 25° and 9° (median values 10° and 3°) for FR I's and normal ellipticals, respectively.

Absolute values of isophote twists as high as those found in the main body ($\mu \sim 21$–23 mag arcsec^{-2}) of the FR I host

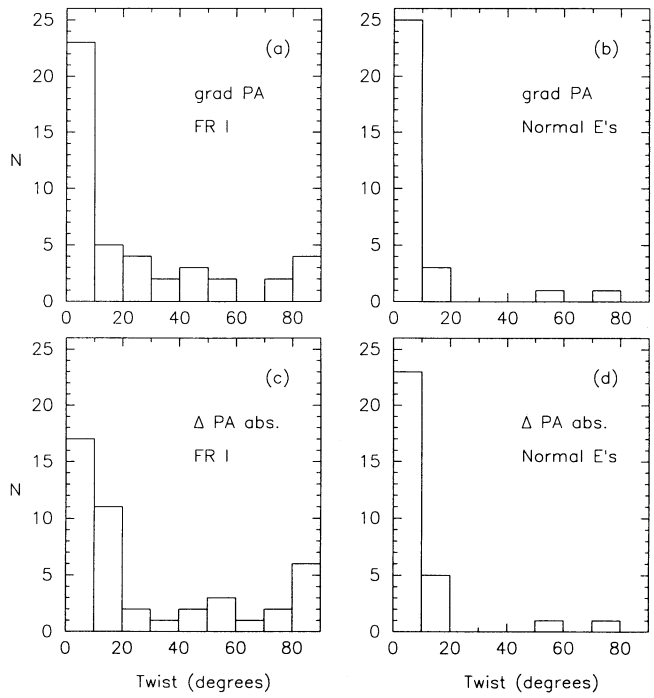

FIG. 1.—(*a*) Distribution of the FR I host galaxies as a function of grad PA (see § 3.1 for details); (*b*) distribution of Sparks sample of nonradio ellipticals as a function of grad PA; (*c*) same as (*a*) but as a function of ΔPA (see § 3.1 for details); (*d*) same as (*b*) but as a function of ΔPA

TABLE 1

THE SAMPLE OF FR I RADIO HOST GALAXIES

Object	cluster	α (1950) (hh mm ss)	δ (1950) (° ′ ″)	z	m_V	M_V	$\log P_{1.4}$ W Hz^{-1}
B2 0034+25	Zw 0034.4+2532	00 34 26.8	+25 25 26	0.0321	13.35	−22.19	23.38
NGC 315	Zw 0107.5+3212	00 55 05.6	+30 04 56	0.0167	12.50	−21.75	24.33
NGC 326	Zw 0056.9+2636	00 55 40.8	+26 35 45	0.0472	13.00	−23.63	24.86
3C 31	Zw 0107.5+3212	01 04 39.2	+32 08 43	0.0169	12.14	−22.07	24.46
NGC 541	A164	01 23 11.2	−01 38 21	0.0181	13.00	−21.32	24.02
NGC 708	A262	01 49 50.0	+35 54 20	0.0160	14.50	−19.64	22.87
4C 35.03	Zw 0216.0+3625	02 06 39.2	+35 33 41	0.0373	13.00	−23.11	24.77
NGC 1044	Zw 0238.4+0831	02 38 25.0	+08 31 24	0.0214	13.27	−21.48	24.05
3C 75	A400	02 55 03.1	+05 49 36	0.0241	13.16	−21.87	24.86
3C 78		03 05 49.1	+03 55 13	0.0288	12.94	−22.49	25.08
NGC 1265	A426	03 14 57.0	+41 40 33	0.0255	12.50	−22.95	25.01
4C 35.16A	A568	07 04 20.0	+35 08 39	0.0780	15.50	−22.42	24.53
4C 53.16	Zw 0712.9+5334	07 12 42.1	+53 28 31	0.0640	15.00	−22.36	25.08
B2 0836+29	A690	08 36 13.4	+29 01 17	0.0790	14.26	−23.24	24.98
B2 0836+29A		08 36 59.1	+29 59 45	0.0650	15.45	−21.76	24.66
B2 0908+37		09 08 45.4	+37 36 33	0.1047	15.67	−22.65	25.09
B2 0915+32		09 15 56.8	+32 03 52	0.0620	15.12	−21.99	24.25
B2 1243+26	A1609	12 43 54.6	+26 43 39	0.0891	15.07	−22.88	24.47
NGC 4789	A1656	12 51 52.3	+27 20 57	0.0270	13.30	−22.04	23.80
NGC 4782/3		12 52 00.1	−12 17 07	0.0138	13.50	−20.35	24.48
B2 1254+27	A1656	12 54 59.4	+27 46 02	0.0249	12.30	−22.74	22.88
NGC 4869	A1656	12 56 58.7	+28 10 51	0.0235	14.90	−19.91	23.14
NGC 5127	Zw 1319.6+3135	13 21 26.3	+31 49 33	0.0161	13.90	−20.18	24.10
B2 1322+36		13 22 35.4	+36 38 19	0.0175	12.84	−21.42	23.67
B2 1357+28		13 57 45.2	+28 44 28	0.0629	14.81	−22.33	24.28
NGC 5490	Zw 1407.6+1750	14 07 37.0	+17 46 48	0.0163	13.40	−20.71	23.93
NGC 5532	A1890	14 14 26.0	+11 02 15	0.0237	12.21	−22.74	24.68
B2 1450+28	A1984	14 50 23.8	+28 10 15	0.1265	16.31	−22.47	24.58
B2 1521+28		15 21 21.4	+28 48 07	0.0825	15.09	−22.68	24.83
B2 1525+29	A2079	15 25 40.5	+29 06 15	0.0653	14.95	−22.27	24.23
B2 1528+29		15 28 05.9	+29 10 43	0.0843	15.35	−22.47	24.46
B2 1553+24		15 53 56.8	+24 35 31	0.0426	14.41	−21.84	23.61
B2 1637+29		16 37 22.2	+29 56 47	0.0875	14.97	−22.94	24.65
B2 1643+27		16 43 26.6	+27 25 30	0.1017	15.77	−22.49	24.03
B2 1658+30		16 58 48.9	+30 12 32	0.0351	14.70	−21.11	24.13
B2 1736+32		17 36 45.2	+32 57 36	0.0741	14.84	−22.67	24.39
B2 1827+32		18 27 04.9	+32 17 59	0.0659	15.10	−22.14	24.32
3C 402 N		19 40 22.5	+50 29 29	0.0247	14.00	−21.37	24.56
NGC 7052		21 16 20.7	+26 14 08	0.0164	14.00	−20.38	22.97
3C 449	Zw 2231.2+3732	22 29 07.7	+39 06 04	0.0171	13.20	−21.28	24.28
B2 2236+35	Zw 2231.2+3732	22 36 12.3	+35 04 11	0.0277	15.00	−20.48	23.65
NGC 7626	Pegaso I	23 18 04.0	+07 57 12	0.0112	12.80	−20.51	23.42
3C 465	A2634	23 35 59.0	+26 45 18	0.0293	15.00	−20.00	25.10
4C 47.63	Zw 2354.1+4719	23 54 57.4	+47 09 39	0.0460	15.00	−21.75	24.88

galaxies need an additional explanation. The fact that most of the galaxies showing these large isophote twist have a close companion or show other evidence of gravitational interactions, supports the hypothesis of Kormendy (1982) in the sense that isophote twist are due not only to triaxiality but also to the effect of tidal forces generated in collisions of galaxies.

3.2. *Nonconcentric Isophotes*

The presence of nonconcentric isophotes is among the strongest evidence of interaction between members of a pair or group of galaxies. Borne (1984) and Aguilar & White (1986) have shown that this kind of morphological characteristic is a short lived transient distortion that arise as a consequence of tidal interactions between galaxies.

The asymmetry in the isophote distribution can be properly quantified by the parameter $\delta = \Delta R/R$ (given in third column of Table 2), where $\Delta R = [(X_c - X_0)^2 + (Y_c - Y_0)^2]^{1/2}$. Here, X_0 and Y_0 represent the position of the center of the inner isophotes (radius less than 5″), while R is the isophotal radius of a selected isophote having X_c and Y_c as center coordinates. The criterium used to select X_c and Y_c is as follows: when either X or Y (or both) have an extreme value (absolute or local), then X_c and/or Y_c correspond to that extreme value (this has been indicated with a mark max/min or local max/min in fourth column of Table 2). When the isophote center is a monotonic function of radius, δ has been evaluated at a radius equal to the effective radius, r_e, or at $2r_e$ if the displacements are detected outside the effective radius. Finally, if sharp discontinuities occur in the stellar distribution (3C 402 N in Table 2), R is the isophotal radius at which these discontinuities appear.

Figure 2 shows the distribution of FR I host galaxies, and Sparks sample as a function of δ. Average values of δ for each distribution are 5.1% and 1.7%, respectively (median values

TABLE 2

TWISTS AND NONCONCENTRIC ISOPHOTES IN FR I HOST GALAXIES

Object	grad PA (degrees)	ΔPA (degrees)	δ (%)	Choice criterion δ
B2 0034+25	28	52	15.0	x_c, local max.
NGC 315	6	6	1.2	r_e
NGC 326 N	90	90	6.4	r_e
3C 31	12	14	3.9	y_c, local max.
NGC 541	60	60	10.4	y_c, min.
NGC 708	50	70	4.0	r_e
4C 35.03	85	85	12.2	x_c, y_c, min.
NGC 1044	35	35	23.7	x_c, max.
3C 75 N	85	85	4.1	x_c, max.
3C 75 S	45	45	7.3	2 r_e
3C 78	4	5	0.9	r_e
NGC 1265	4	4	3.5	r_e
4C 35.16A	21	21	4.1	r_e
4C 53.16	6	9	4.5	r_e
B2 0836+29	17	18	7.3	2 r_e
B2 0836+29A	54	85	4.2	y_c, min.
B2 0908+37	9	10	3.0	r_e
B2 0915+32	80	90	0.3	2 r_e
B2 1243+26	50	77	1.5	2 r_e
NGC 4789	5	5	1.1	r_e
NGC 4782	11	13	16.8	r_e
B2 1254+27	2	3	1.7	2 r_e
NGC 4869	26	45	1.4	r_e
NGC 5127	2	2	1.8	r_e
B2 1322+36	5	10	2.4	2 r_e
B2 1357+28	16	16	5.0	x_c, local min.
NGC 5490	7	13	0.9	r_e
NGC 5532	7	12	1.4	r_e
B2 1450+28	10	10	16.4	r_e
B2 1521+28	4	4	1.5	2 r_e
B2 1525+29	26	30	3.5	2 r_e
B2 1528+29	80	80	2.3	2 r_e
B2 1553+24	4	11	1.1	r_e
B2 1637+29	3	5	6.3	y_c, local max.
B2 1643+27	10	20	1.8	r_e
B2 1658+30	5	10	1.2	2 r_e
B2 1736+32	8	10	*	*
B2 1827+32	10	10	1.3	r_e
3C 402 N	82	82	5.7	discontinuities
NGC 7052	4	5	3.1	r_e
3C 449	35	60	14.6	r_e
B2 2236+35	16	17	6.2	r_e
NGC 7626	6	11	2.3	r_e
3C 465	5	8	6.2	r_e
4C 47.63	10	14	1.2	r_e

NOTES.—(*) Parameters affected by the presence of a saturated star.

3.5% and 1.5%). From these histograms it is clearly seen that FR I host galaxies are more widely distributed over δ and show much larger values of δ than nonradio ellipticals.

Assuming that galaxies with nonconcentric isophotes must have $\delta \geq 3.5\%$ (twice the average value found for Sparks sample) we then find that a fraction as large as 52% of FR Is shows displacements in excess of 3.5%. In Sparks's sample, this fraction decreases down to 17%. Moreover, Lauer (1985) found no evidence of nonconcentric isophotes in a sample of 42 normal ellipticals. An average upper limit of $\delta = 0.5\%$ over the inner 5 kpc was obtained for that sample of galaxies.

However, some of the bright cluster galaxies in the Lauer (1988) multiple-nucleus galaxy sample show δ values larger than 10%. In the present sample we find values of δ as large as 15%–25% in pair of galaxies with a close distorted companion (B2 0034+25, NGC 1044, NGC 4782/4783, B2 1450+28, 3C 449). This stresses the hypothesis of Borne (1984) and Aguilar & White (1986) that isophote displacements originate in the presence of tidal forces in recent, close and strong collisional encounters.

3.3. *Departures from a de Vaucouleurs Luminosity Profile*

A de Vaucouleurs law has been fitted to the light profile of all the galaxies in the sample. The law fitted to the entire extent of the profile is not usually the best fit, because the profile shows bumps and wiggles at intermediate radius around the fitted $r^{1/4}$ law. In such cases, a new $r^{1/4}$ law has been fitted typically over the inner $\sim 3''$–$10''$ region of the profile, and departures from this new law in the form of a light excess appear at isophotal radii beyond r_e (see Fig. 6 in the appendix to visualize the radial dependence of the light excess for each galaxy).

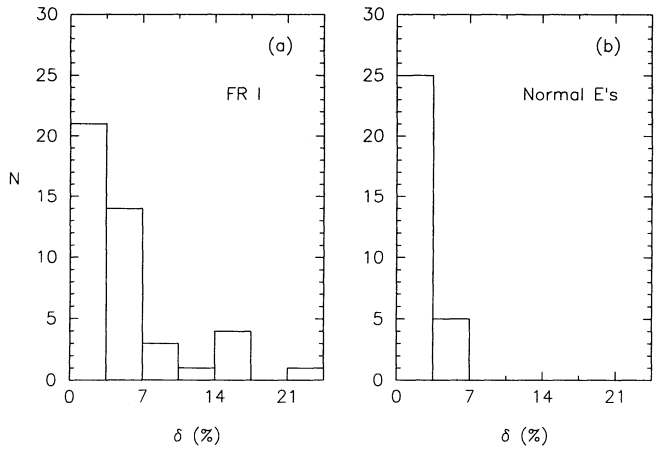

FIG. 2.—(*a*) Distribution of the FR I host galaxies as a function of parameter δ (see § 3.2 for details); (*b*) same as (*a*) but for Sparks sample of nonradio ellipticals.

To evaluate the excess, the parameters of the best $r^{1/4}$ law fit (effective magnitude, μ_e, and radius, r_e, in Table 3) over the inner radii (columns labeled r_{min} and r_{max} in Table 3 indicate the limiting radii for the fit) have been derived. The amount of excess is represented by the difference between fitted and observed magnitudes at radii equal to $2r_e$ and $3r_e$ [columns labeled $\Delta\mu(2r_e)$ and $\Delta\mu(3r_e)$ in Table 3]. We also define an "excess radius," r_{excess}, as the radius at which light profile begins to depart from the $r^{1/4}$ law by more than 0.05 mag arcsec^{-2}. Light excess above a $r^{1/4}$ law has been detected in 73% (33/45) of the sample. On the average, the measured excess at $2r_e$ and $3r_e$ are about 0.37 and 0.57 mag arcsec^{-2}, respectively.

The fraction of FR I host galaxies showing light excess is similar to the fraction of bright multiple-nucleus cluster galaxies presenting departures from a de Vaucouleurs law. Lauer (1988) presented luminosity profiles for 17 multiple-nucleus brightest cluster galaxies. If we apply the criteria for defining light excess to the galaxies of Lauer's sample, at least 65% of them showed departures from a $r^{1/4}$ law.

The amount of light excess in FR I host galaxies is similar to that found in cD galaxies, which show departures from a de Vaucouleurs law at large isophotal radius (Schombert 1986). We estimate the amount of excess for the 27 cDs of the Schombert sample of the brightest cluster galaxies (Schombert 1988) to be $\sim$0.50 mag arcsec^{-2} and $\sim$0.70 mag arcsec^{-2} at $2r_e$ and $3r_e$, respectively. Although the light excess in cD galaxies is interpreted as evidence of a halo probably formed both by successive events of mergers or by tidal interactions between cluster members (see Kormendy & Djorgvorski 1989, and references therein), not all of the few galaxies of the present sample classified as cD show a large excess over the $r^{1/4}$ law. For instance B2 0836+29, B2 1254+27, and 3C 465 do while NGC 708 and 3C 75 do not. Also, there is a substantial difference between the excess detected in FR I host galaxies and in cD galaxies. While light excess in the halos of cD galaxies are

TABLE 3

FR I HOST GALAXIES WITH EXCESSES OVER THE $r^{1/4}$ LAW

Object	r_{min} (")	r_{max} (")	μ_e ($mag/arcsec^2$)	r_e (")	r_e (kpc)	r_{excess} (")	r_{excess} (kpc)	$\Delta\mu\,(2r_e)$ ($mag/arcsec^2$)	$\Delta\mu\,(3r_e)$ ($mag/arcsec^2$)
B2 0034+25	4.1	6.5	21.54 ± 0.06	8.4 ± 0.3	5.2 ± 0.2	6.9	4.3	0.59	0.97
NGC 326 N	1.9	4.98	21.17 ± 0.06	5.5 ± 0.2	5.0 ± 0.2	5.4	4.9	0.42	0.66
3C 31	5.0	17.9	21.03 ± 0.04	15.8 ± 0.3	5.2 ± 0.1	18.7	6.1	0.31	0.53
NGC 541	1.8	12.2	21.39 ± 0.04	13.3 ± 0.3	4.7 ± 0.1	13.3	4.7	0.57	0.78
4C 35.03	2.0	4.8	19.80 ± 0.07	4.1 ± 0.2	3.0 ± 0.1	5.0	3.6	0.49	0.98
NGC 1044	1.9	5.7	21.41 ± 0.05	9.9 ± 0.3	4.1 ± 0.1	6.2	2.6	0.47	0.69
3C 75 N	2.4	13.0	20.72 ± 0.04	6.0 ± 0.1	2.8 ± 0.1	14.6	6.8	–	0.22
3C 75 S	2.6	7.3	21.06 ± 0.04	6.4 ± 0.1	3.0 ± 0.1	8.8	4.1	0.16	0.30
3C 78	1.8	11.6	21.99 ± 0.03	15.1 ± 0.2	8.4 ± 0.1	12.6	7.0	0.21	0.28
NGC 1265	2.5	10.3	21.59 ± 0.04	13.3 ± 0.3	6.6 ± 0.2	11.8	5.8	0.36	0.47
4C 35.16A	1.7	4.5	21.24 ± 0.06	3.7 ± 0.1	5.6 ± 0.2	4.7	7.0	0.23	0.50
B2 0836+29	2.4	5.3	22.53 ± 0.04	9.1 ± 0.2	13.9 ± 0.3	6.3	9.6	0.74	1.19
B2 0915+32	2.2	4.7	21.34 ± 0.04	4.2 ± 0.1	5.0 ± 0.1	5.2	6.2	0.30	0.59
B2 1243+26	2.3	6.1	21.27 ± 0.04	4.2 ± 0.1	7.2 ± 0.2	6.6	11.3	0.18	0.43
NGC 4789	2.2	10.5	21.36 ± 0.02	13.7 ± 0.1	7.2 ± 0.1	11.1	5.8	0.24	0.53
NGC 4782	2.9	6.8	20.50 ± 0.10	13.1 ± 1.2	3.5 ± 0.3	7.0	1.9	0.35	0.83
B2 1254+27	2.0	8.9	22.28 ± 0.01	20.4 ± 0.2	9.9 ± 0.1	10.9	5.3	0.58	0.59
B2 1322+36	2.8	8.7	19.96 ± 0.05	8.4 ± 0.2	2.9 ± 0.1	9.7	3.3	0.22	0.42
B2 1357+28	1.8	5.2	21.88 ± 0.02	5.7 ± 0.1	6.9 ± 0.1	5.8	7.1	0.42	0.65
NGC 5490	3.5	17.4	20.42 ± 0.01	10.4 ± 0.1	3.3 ± 0.0	21.7	6.9	–	0.21
B2 1450+28	1.9	5.1	22.51 ± 0.10	4.5 ± 0.2	11.6 ± 0.6	5.3	13.0	0.48	0.44
B2 1521+28	1.7	5.2	22.13 ± 0.03	5.5 ± 0.1	8.8 ± 0.1	5.8	9.3	0.34	0.57
B2 1525+29	2.4	5.0	20.58 ± 0.07	2.9 ± 0.1	3.6 ± 0.1	5.5	6.9	0.05	0.33
B2 1553+24	2.1	6.7	21.83 ± 0.02	7.4 ± 0.1	6.1 ± 0.1	7.4	6.1	0.34	–
B2 1637+29	2.0	9.1	21.84 ± 0.08	6.9 ± 0.2	11.8 ± 0.4	5.6	9.5	0.35	0.44
B2 1658+30	1.8	7.0	21.01 ± 0.05	3.7 ± 0.1	2.5 ± 0.1	7.1	4.8	0.09	0.43
B2 1827+32	1.5	4.2	22.65 ± 0.04	7.1 ± 0.2	9.0 ± 0.2	4.4	5.7	0.27	0.62
3C 402 N	2.3	7.8	20.47 ± 0.03	9.0 ± 0.2	4.3 ± 0.1	8.9	4.2	0.38	0.57
3C 449	2.0	5.6	20.50 ± 0.03	7.3 ± 0.1	2.4 ± 0.0	6.8	2.3	0.27	0.38
B2 2236+35	1.2	15.0	22.28 ± 0.03	17.9 ± 0.3	9.6 ± 0.2	15.4	8.3	0.45	0.65
NGC 7626	2.4	7.1	21.30 ± 0.06	22.1 ± 0.9	4.8 ± 0.2	8.0	1.7	0.41	0.17
3C 465	1.7	9.6	21.35 ± 0.04	10.9 ± 0.3	6.2 ± 0.2	9.5	5.4	0.59	0.99
4C 47.63	1.5	5.4	21.84 ± 0.03	8.4 ± 0.1	7.5 ± 0.1	5.9	5.2	0.50	0.75

observed beyond a surface brightness of 24 mag arcsec^{-2} (Schombert 1988), FR I host galaxies show a light excess at a much higher surface brightness ($\mu \sim 22 - 23$ mag arcsec^{-2}), well inside the main optical body of the galaxy (see Fig. 6 in the appendix).

3.4. *Presence of Close Companion Galaxies*

We consider here as close companions those galaxies within a radius of 50 kpc from the FR I host galaxy. Most of the companions show at least one indication of being disrupted by tidal effects (twist, nonconcentric isophotes, light excess). Considering that criterion, 47% (21/45) of FR I host galaxies in the sample show a close companion. These galaxies are marked with "Y" in fifth column of Table 4.

Two other galaxies (B2 1254+27, NGC 5532) have a small companion at less than 50 kpc but without any clear signature of interaction with the main galaxy. Since a large fraction of FR I host galaxies are located in clusters, there is a non-negligible chance (~13%; see Colina & Pérez-Fournon 1990b) of having pairs produced by line-of-sight spurious superpositions without being in physical interaction. The small companion galaxies around B2 1254+27 and NGC 5532 could, most likely, be examples of such a situation since the B2 1254+27 and NGC 5532 host galaxies are located in clusters (see Table 1).

TABLE 4

EVIDENCE FOR INTERACTION IN FR I HOST GALAXIES

Object	Twist	Isophote displ.	Excess	Close comp.	Interaction likehood (%)
B2 0034+25	Y	Y	Y	Y	100
NGC 315	N	N	N	N	0
NGC 326 N	Y	Y	Y	Y	100
3C 31	N	Y	Y	Y	75
NGC 541	Y	Y	Y	N	75
NGC 708	Y	Y	N	Y	75
4C 35.03	Y	Y	Y	Y	100
NGC 1044	Y	Y	Y	Y	100
3C 75 N	Y	Y	Y	Y	100
3C 75 S	Y	Y	Y	Y	100
3C 78	N	N	Y	N	25
NGC 1265	N	Y	Y	N	50
4C 35.16A	Y	Y	Y	Y	100
4C 53.16	N	Y	N	Y	50
B2 0836+29	Y	Y	Y	N	75
B2 0836+29A	Y	Y	N	N	50
B2 0908+37	N	N	N	N	0
B2 0915+32	Y	N	Y	Y	75
B2 1243+26	Y	N	Y	N	50
NGC 4789	N	N	Y	N	25
NGC 4782/3	N	Y	Y	Y	75
B2 1254+27	N	N	Y	Y?	25
NGC 4869	Y	N	N	N	25
NGC 5127	N	N	N	N	0
B2 1322+36	N	N	Y	Y	50
B2 1357+28	Y	Y	Y	N	75
NGC 5490	N	N	Y	N	25
NGC 5532	N	N	N	Y?	0
B2 1450+28	N	Y	Y	Y	75
B2 1521+28	N	N	Y	N	25
B2 1525+29	Y	Y	Y	Y	100
B2 1528+29	Y	N	N	N	25
B2 1553+24	N	N	Y	N	25
B2 1637+29	N	Y	Y	Y	75
B2 1643+27	N	N	N	N	0
B2 1658+30	N	N	Y	N	25
B2 1736+32	N	*	*	N	≤50
B2 1827+32	N	N	Y	N	25
3C 402 N	Y	Y	Y	Y	100
NGC 7052	N	N	N	N	0
3C 449	Y	Y	Y	Y	100
B2 2236+35	Y	Y	Y	Y	100
NGC 7626	N	N	Y	N	25
3C 465	N	Y	Y	Y	75
4C 47.63	N	N	Y	Y	50

NOTES.—(*) Parameters affected by the presence of a saturated star.

3.5. *Overall Evidence of Gravitational Interaction*

This section summarizes the peculiarities found in the sample: isophote twist, nonconcentric isophotes, light excess, and presence of a close companion. Table 4 gives a summary of these four effects, marking for each galaxy the presence, or not, of a given feature with a "Y" (yes) or "N" (no) in the corresponding column. The criteria used to award a "Y" are the following: (1) isophote twists equal or larger than 15°, (2) isophote displacements characterized by the parameter δ equal or larger than 3.5%, (3) light excess above a $r^{1/4}$ of at least 0.10 mag arcsec^{-2} at distances beyond an effective radius, and (4) presence of a companion galaxy at a distance equal to or less than 50 kpc and with at least one peculiar morphological feature. All these criteria represent values that are well above the average values measured in samples of standard galaxies. Therefore, the fraction of spurious line-of-sight pairs non-physically interacting is zero, or close to zero.

The column labeled "interaction likelihood" assigns an "interaction percentage" to each galaxy according to the number of "Y" given in previous columns. We consider the presence of at least two of the four morphological distortions (interaction percentage $\geq 50\%$) as evidence that a gravitational interaction has taken place.

Considering the interaction percentage defined above, at least 60% (27/45) of the present sample of FR I galaxies is experiencing (or has experienced) a strong recent collision. This fraction is still 47% if the presence of at least three of the above mentioned gravitational effects are considered as evidence of a recent collision.

Some of the galaxies (NGC 541, NGC 1265, B2 0836+29A, B2 1243+36, B2 1357+28) are classified as interacting systems, although they have no interacting companions at distances of less than 50 kpc. However, in those cases, the FR I host galaxy presents additional features (like the radio structure; see comments on González-Serrano et al. 1993, de Juan et al. 1994) suggesting that they might be interacting with galaxies located further out, i.e., at distances larger than 50 kpc from the radio galaxy, or that they are examples of older collisions.

Although a complete and exhaustive analysis like the one presented here has never been attempted with samples of normal ellipticals, we have shown that the fraction of non-radio ellipticals having any of the mentioned distortions is very much lower than for FR I host ellipticals. Despite other considerations about the generation of the radio source not yet analyzed here (see § 5; influence of the ISM: de Juan 1994; de Juan & Colina 1995), it can be concluded that gravitational collisions between ellipticals play a key role in triggering a FR I radio source in the nucleus of bright ellipticals.

4. FR I HOST GALAXIES: CHARACTERIZATION OF THE COLLISION

It is already known that FR I radio host galaxies inhabit regions characterized by local galaxy densities larger than

those found around radio quiet ellipticals and FR II radio host galaxies (see detailed studies by Longair & Seldner 1979; Heckman, Carty & Bothun 1985; Lilly & Prestage 1987; González-Serrano et al. 1993). A large fraction (61%) of the galaxies in our sample are members of Abell or Zwicky clusters. The rest of the galaxies are usually bright galaxies located in a small group of galaxies. In the dense environments of groups or clusters, collisions can occur at a larger rate than in other more scarce regions activating the radio source. The gravitational interactions generated during a collision would help the gas and/or stars to fall into the deep potential of a bright elliptical, and generate ultimately a FR I radio source. In the following we present a quantitative and physical characterization of FR I host galaxies involved in a collision. This approach is a first step toward a more detailed and quantitative study of the causal connection between collisions of galaxies and the onset of activity in their nuclei.

TABLE 5A

PHOTOMETRIC PROPERTIES OF FR I HOST GALAXIES

Name	Ellipticity	μ_e mag arcsec^{-2}	±	r_e (kpc)	±
B2 0034+25	0.27	22.85	0.04	22.7	0.4
NGC 315	0.26	21.72	0.06	10.2	0.3
NGC 326 N	0.08	22.17	0.09	9.2	0.5
3C 31	0.14	21.03	0.04	5.2	0.1
NGC 541	0.11	21.39	0.04	4.7	0.1
NGC 708	0.28	22.15	0.03	8.6	0.1
4C 35.03	0.06	23.44	0.05	25.6	0.8
NGC 1044	0.11	22.33	0.05	7.5	0.2
3C 75 N	0.07	20.72	0.04	2.8	0.1
3C 75 S	0.03	21.62	0.06	4.1	0.1
3C 78	0.25	22.35	0.03	10.8	0.2
NGC1265	0.24	22.26	0.05	10.0	0.2
4C 35.16A	0.06	22.28	0.09	10.1	0.5
4C 53.16	0.32	23.36	0.03	26.4	0.4
B2 0836+29	0.09	22.22	0.03	11.8	0.2
B2 0836+29A	0.16	24.90	0.06	38.0	1.7
B2 0908+37	0.31	23.60	0.05	21.7	0.7
B2 0915+32	0.05	21.47	0.09	5.5	0.3
B2 1243+26	0.11	21.38	0.04	7.5	0.2
NGC 4789	0.31	21.76	0.04	9.3	0.2
NGC 4782	0.24	21.24	0.03	5.7	0.1
B2 1254+27	0.36	22.44	0.03	10.2	0.3
NGC 4869	0.13	21.03	0.05	3.3	0.1
NGC 5127	0.24	22.39	0.03	7.9	0.1
B2 1322+36	0.30	20.71	0.02	2.9	0.0
B2 1357+28	0.08	22.06	0.05	7.7	0.2
NGC 5490	0.16	20.93	0.07	4.3	0.1
NGC 5532	0.17	21.31	0.02	8.2	0.1
B2 1450+28	0.25	22.65	0.13	11.8	1.0
B2 1521+28	0.16	22.23	0.06	9.2	0.3
B2 1525+29	0.09	21.16	0.05	5.0	0.1
B2 1528+29	0.18	22.02	0.06	8.9	0.3
B2 1553+24	0.35	22.36	0.06	7.6	0.4
B2 1637+29	0.33	22.52	0.08	18.0	1.1
B2 1643+27	0.17	23.50	0.04	17.9	0.5
B2 1658+30	0.11	20.60	0.05	2.1	0.1
B2 1736+32	0.29	23.03	0.09	19.6	1.5
B2 1827+32	0.08	22.74	0.03	11.0	0.2
3C 402N	0.07	20.47	0.03	4.3	0.1
NGC 7052	0.53	21.94	0.03	8.5	0.1
3C 449	0.20	21.19	0.04	3.6	0.0
B2 2236+35	0.15	22.41	0.04	10.5	0.2
NGC 7626	0.17	21.95	0.03	7.6	0.1
3C 465	0.26	21.66	0.08	7.6	0.3
4C 47.63	0.09	22.44	0.08	11.2	0.6

4.1. *Type of Ellipticals*

The FR I radio host galaxies and close companions are characterized here by their effective magnitude (μ_e)-radius (r_e) relationship, and by their ellipticity (ϵ).

4.1.1. *The $\mu_e - r_e$ Relation*

The effective magnitude and radius for FR I host galaxies and companions can be found in Table 5A and Table 5B, respectively. To standardize the comparison with other sample of galaxies, the effective magnitude and radius presented in Tables 5A and 5B are obtained by fitting the light profile over its whole extent to a de Vaucouleurs law. Thus, for those FR I host galaxies presenting a light excess over the $r^{1/4}$ law, the parameters μ_e and r_e in Table 5A differ from that on Table 3.

FR I host galaxies are well differentiated from their companions. FR I galaxies are bright ellipticals with average effective brightness and radius $\mu_e = 22.1 \pm 0.9$ mags arcsec^{-2} and $r_e = 10.5 \pm 7.2$ kpc, respectively. Companion galaxies are, in general, smaller compact ellipticals with average brightness and radius $\mu_e = 20.7 \pm 1.3$ mags arcsec^{-2} and $r_e = 4.0 \pm 4.2$ kpc, respectively.

The $\mu_e - r_e$ relation obtained for FR I radio sources is given by

$$\text{FR I: } \mu_e(r \text{ mag arcsec}^{-2}) = 3.03(\pm 0.19) \log r_e(\text{kpc}) + 19.23(\pm 0.18) . \quad (1)$$

This relation (see Fig. 3) is similar to the $\mu_e - r_e$ relation obtained for ellipticals (Kormendy 1977), and slightly different from the one obtained for the brightest ellipticals in Abell clusters (BCG: Hoessel, Oegerle, & Schneider 1987), which respectively follow the relations:

$$\text{Ellipticals: } \mu_e = 3.01(\pm 0.28) \log r_e + 19.14(\pm 0.19) , \quad (2)$$

$$\text{BCGs: } \mu_e = 3.14(\pm 0.09) \log r_e + 18.94(\pm 0.13) . \quad (3)$$

The differences in the $\mu_e - r_e$ relation between FR I radio host galaxies and BCGs are in the sense that, for a given effec-

TABLE 5B

PHOTOMETRIC PROPERTIES OF FR I COMPANIONS GALAXIES

Name	Ellipticity	μ_e mag arcsec^{-2}	±	r_e (kpc)	±
B2 0034+25	0.23	21.12	0.11	2.0	0.1
NGC 326 S	0.16	21.99	0.07	7.7	0.3
3C 31	0.05	18.60	0.10	0.8	0.0
4C 35.03	0.09	21.16	0.09	3.2	0.1
NGC 1044	0.10	17.96	0.07	0.5	0.0
3C 75 N	0.02	20.72	0.04	2.8	0.1
3C 75 S	0.04	21.62	0.06	4.1	0.1
4C 35.16A-1	0.26	21.72	0.05	10.8	0.3
4C 35.16A-2	0.07	20.70	0.10	4.4	0.3
4C 53.16	0.03	18.60	0.10	1.0	0.0
B2 0915+32	0.22	22.00	0.09	4.7	0.2
NGC 4783	0.25	21.08	0.06	3.9	0.1
B2 1322+36	0.45	19.55	0.04	1.9	0.0
NGC 5532	0.30	18.40	0.10	0.8	0.0
B2 1450+28	0.02	21.01	0.09	4.7	0.2
B2 1525+29	0.36	22.94	0.04	18.9	0.5
B2 1637+29	0.15	22.41	0.08	5.2	0.2
3C 402N-1	0.54	19.96	0.13	0.9	0.0
3C 402N-2	0.39	20.11	0.08	1.6	0.1
3C 449	0.17	19.54	0.05	0.7	0.0
B2 2236+35	0.04	20.88	–	2.7	–
3C465	0.30	20.11	0.05	1.6	0.0

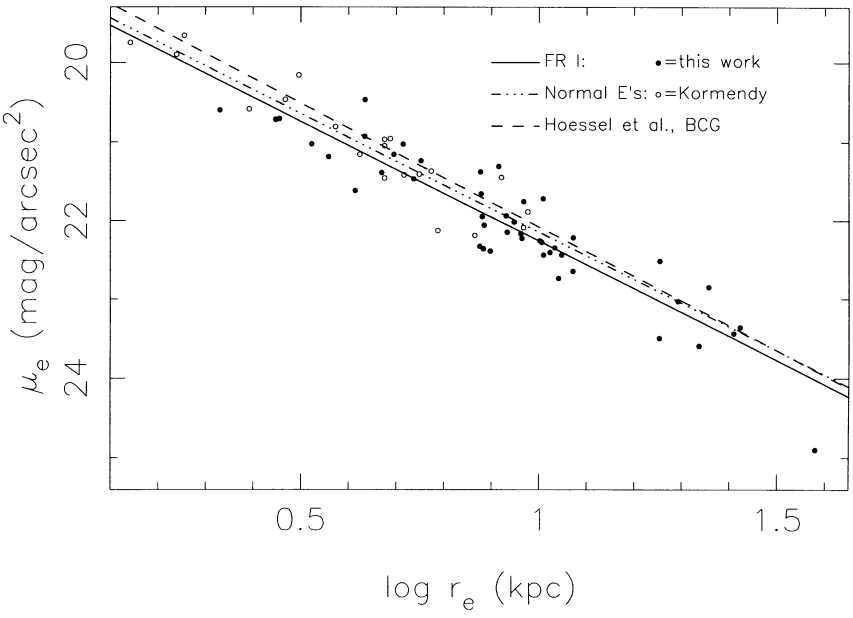

FIG. 3.—$\mu_e - r_e$ relation for the sample of FR I host galaxies, normal ellipticals and brightest cluster galaxies (see § 4.1.1 for details)

tive radius, BCGs are brighter than FR I host galaxies. This differentiation could reflect the fact that although FR I galaxies are bright ellipticals preferentially located in groups and clusters of galaxies, only a small fraction of the FR I sources appears to be associated with the brightest galaxy of a cluster.

We now turn to the companions of FR I host galaxies. Close companions are normal ellipticals and differ substantially from the fainter galaxies in clusters as measured by Hoessel et al. (1987). The $\mu_e - r_e$ relations obtained for the fainter galaxies in clusters (Fainter-CG) and for the close companions around FR I radio host galaxies (Comp-FR I) are given by

$$\text{Fainter-CG: } \mu_e = 4.56(\pm 0.14) \log r_e + 19.10(\pm 0.11)\,, \quad (4)$$

$$\text{Comp-FR I: } \mu_e = 2.93(\pm 0.31) \log r_e + 19.42(\pm 0.18)\,. \quad (5)$$

The discrepancy in the $\mu_e - r_e$ relation between the Fainter-CG and the FR I companion galaxies could be real. Many of the FR I companion galaxies are also bright ellipticals with a size and mass similar to that of the FR I host galaxy (i.e., dumbbell systems like in NGC 326, 3C 75, and NGC 4782/4783). However, the discrepancy could also be an artifact generated by seeing related effects. Fainter-CG galaxies are small compact ellipticals where the effective radius is small compared to the seeing disk, therefore producing a steeper $\mu_e - r_e$ relation.

4.1.2. *The Ellipticity Distribution*

The second parameter, i.e., the characteristic ellipticity for the FR I host galaxies, has been measured at r_e (see Table 5A). For the FR I companion galaxies the ellipticity has been measured at a distance of $2r_e$ (see Table 5B) in an effort to minimize seeing effects that would produce observed shapes rounder than the intrinsic ones.

FR I host galaxies show an ellipticity distribution with a slight tendency to be rounder, on average than cluster ellipticals (Fig. 4*a* and 4*d*; original sample by Strom and Strom as referred in Smith & Heckman 1989a). Although this result could confirm previous claims that radio host galaxies are round ellipticals (Disney, Sparks, & Wall 1984), results for a larger sample are needed to obtain a statistical confirmation. On the other hand, galaxies associated with powerful radio sources (most FR IIs) follow the same ellipticity distribution as ellipticals (Smith & Heckman 1989a and references therein; see also Figure 4*c*). As already suggested by Smith & Heckman, the difference in the ellipticity distribution among low lumi-

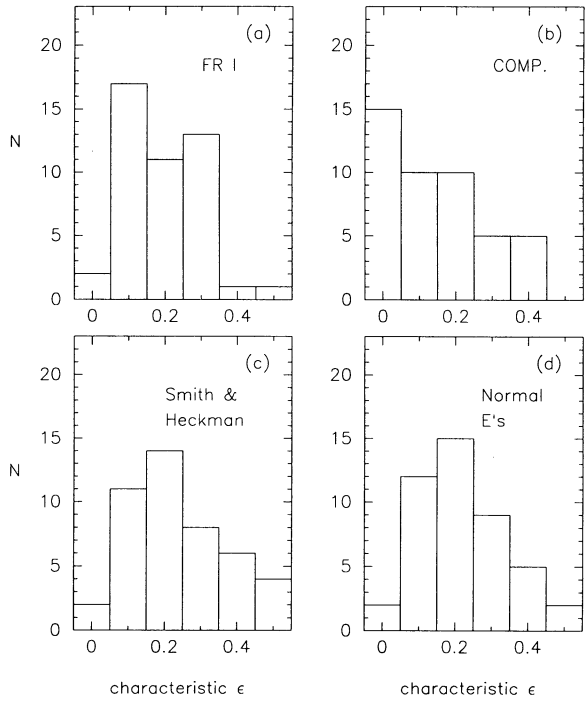

FIG. 4.—(*a*) Distribution of the FR I host galaxies as a function of observed ellipticity; (*b*) same as (*a*) but for the FR I companion galaxies; (*c*) same as (*a*) but for Smith & Heckman sample of powerful radio host galaxies; (*d*) same as (*a*) but for cluster ellipticals as referred in Smith & Heckman (1989a). The distribution of all samples have been normalized to the total number of galaxies in the FR I sample. See § 4.1.2 for details.

nosity (FR I) and high luminosity (FR II) radio host galaxies, if real, could indicate a close relation between the kind of activity generated in the nucleus of an elliptical and its morphological type.

FR I companion galaxies have an ellipticity distribution with an excess of round ellipticals when compared with normal ellipticals (see Fig. 4*b*). We believe that the seeing still affect the ellipticity distribution of these more compact and smaller galaxies, producing artificially rounder isophotes.

4.2. *Mass Ratio, Distance and Relative Velocities of the Colliding Galaxies*

The mass ratio of the ellipticals involved in the collision can be calculated considering the expression $L = 7.22\pi r_e^2 I_e$ (Mihalas & Binney 1981), and assuming a mass-to-light ratio $M/L \propto L^{0.35}$ (Kormendy & Djorgovski 1989). Doing some algebra, the mass ratio is obtained as a function of the observed effective magnitude (μ_e) and radius (r_e) by

$$\log (M_c/M_R) = 2.7 \log (r_e^c/r_e^R) + 0.54(\mu_e^R - \mu_e^c) . \quad (6)$$

In this expression the subscripts "c" and "R" refer to the companion and radio host galaxy parameters listed in Table 5A and 5B, respectively. The results for each galaxy pair can be found in Table 6. Typical pair mass ratios are in the 0.1 to 1.0 range although more extreme cases of small (B2 0034+25) or large (4C 35.16A and B2 1322+36) companions are also observed.

The linear projected separation of the galaxies involved in the collision are measured directly from the angular separation of their centers. Many (14/21) of the collisions are deep encounters with projected separations of less than 30 kpc. The relative velocities of the pair galaxies are obtained from data already published (see references in Table 6).

The collision can be characterized by (1) a median mass ratio (companion to FR I host galaxy) of $M_c/M_R = 0.2$, (2) a median projected distance of 23 kpc, and (3) a median relative velocity of $\Delta V = 492$ km s^{-1}.

TABLE 6

CHARACTERIZATION OF THE COLLISION OF FR I HOST GALAXIES

Name	M_c/M_R	Distance kpc	ΔV km s^{-1}	Ref.
B2 0034+25	0.02	26.0	–	–
NGC 326	0.77	6.5	750	1
3C 31	0.14	10.9	129	2
NGC 708*	~ 0.2	20.5	–	–
4C 35.03	0.06	30.4	70	1
NGC 1044	0.15	7.7	185	1
3C 75 N	0.91	7.6	354	1
3C 75 S	1.09	7.6	354	1
4C 35.16A-1	2.40	35.0	–	–
4C 35.16A-2	0.76	45.4	–	–
4C 53.16	0.05	27.4	–	–
B2 0915+32	0.34	42.0	–	–
NGC 4782	0.44	10.8	637	1
B2 1322+36	1.33	47.3	53	3
B2 1450+28	0.64	23.6	1000	1
B2 1525+29	16.4	48.8	20	1
B2 1637+29	0.04	11.1	4100	4
3C 402N-1	0.03	17.5	630	5
3C 402N-2	0.10	23.2	929	5
3C 449	0.10	12.4	80	6
B2 2236+35	0.10	47.0	–	–
3C 465	0.10	6.9	997	1
4C 47.63*	~0.2	35.8	–	–

NOTES.—(*) The mass ratio M_c/M_R has been estimated measuring the diameter (D) of the galaxies and considering a $D^{1.5}$ dependence for the mass

REFERENCES.—(1) Valentjin & Casertano 1988; (2) Colina & Borne, unpublished; (3) Soares 1989; (4) de Ruiter et al. 1988; (5) Colina, unpublished; (6) Wirth et al. 1982.

4.3. *Age of the Collision*

An estimate of the time elapsed since closest approach can be derived by measuring the short transient effects that a collision produces in the stellar distribution of a galaxy. There are two main effects: (1) the presence of displacements in the isophotes, i.e., nonconcentric isophotes, and (2) the existence of an excess above a de Vaucouleurs law in the luminosity profile.

The presence of nonconcentric isophotes is produced by the fact that the nucleus of a galaxy reacts as a solid body to the gravitational interaction, i.e., it moves as a whole from its previous equilibrium position, while the intermediate and outer regions are affected by differential tidal effects (Borne 1984; Aguilar & White 1986). However, since the dynamical friction is very efficient in moving the nucleus back to the center of the surrounding envelope, the presence of displaced isophotes in the inner regions of galaxies is a short-lived transient effect (Lauer 1988). An estimation of time elapsed since the gravitational encounter started can be obtained by measuring the radius at which the observed isophote displacement is detected.

$$t_{\rm isophot} = 2 \times r_{\rm nonconc} \times \sigma^{-1} = 1.96 \times 10^9 \times r_{\rm nonconc} \times \sigma^{-1} \text{ yr} , \quad (7)$$

where $r_{\rm nonconc}$ is the radius (in kpc) at which non-concentric isophotes are detected, and σ is the velocity dispersion in km s^{-1}. For the galaxies in our sample, $r_{\rm nonconc}$ is the distance at which the isophote displacement becomes larger than 3.5% according to the δ parameter defined in § 3.2, (see Table 7). Considering a velocity dispersion of 250 km s^{-1} as a standard value for bright ellipticals, the time since the interaction began is $t_{\rm isophot} \sim 2 \times 10^7$–$2 \times 10^8$ yrs for the FR I colliding galaxies (see Table 7).

The early detection (Kormendy 1977) of luminosity excess in the outer regions of ellipticals above a de Vaucouleurs law was interpreted as a consequence of tidal effects (Kormendy 1977, 1982). More recent numerical simulations by Aguilar & White (1986) indicate that such luminosity excesses as those detected by Kormendy are transient phenomena occurring during the collision of two ellipticals. Aguilar & White (1986) demonstrate that the radius at which the luminosity excess appears can be related to the time elapsed since closest approach, independently of the physical parameters of the collision. Therefore, a second and independent estimate of the time elapsed since closest approach can be obtained by calculating the radius ($r_{\rm excess}$) at which the luminosity excess appears in the FR I host galaxy:

$$t_{\rm profile} = 2 \times r_{\rm excess} \times \sigma^{-1} = 1.96 \times 10^9 \times r_{\rm excess} \times \sigma^{-1} \text{ yr} , \quad (8)$$

where σ is the velocity dispersion in km s^{-1}, and $r_{\rm excess}$ is the radius (in kpc) at which the excess above the extrapolation of a de Vaucouleurs law for the internal isophotes is determined (see § 3.3 and Table 3). For the galaxies in this sample, a $t_{\rm profile}$ within the range 2×10^7–10^8 yrs, is obtained assuming $\sigma = 250$ km s^{-1} (see Table 7).

TABLE 7

AGE OF THE COLLISION OF FR I HOST GALAXIES

Name	$r_{nonconc}$ kpc	$t_{isophot}$ 10^7 yrs	r_{excess} kpc	$t_{profile}$ 10^7 yrs	t_{age} 10^8 yrs	IS
B2 0034+25	5.2	4.1	4.3	3.4	0.38	3.5×10^{-3}
NGC 326	8.2	6.4	4.9	3.8	0.51	$1.1\times10^{+1}$
3C 31	9.5	7.4	6.1	4.8	0.61	5.3×10^{-1}
NGC 708	4.2	3.3	–	–	0.33	$\sim 9\times10^{-2}$
4C 35.03	5.5	4.3	3.6	2.8	0.36	6.2×10^{-3}
NGC 1044	2.1	1.6	2.6	2.0	0.18	4.7×10^{-1}
3C 75 N	6.7	5.3	6.8	5.3	0.53	$8.8\times10^{+0}$
3C 75 S	4.4	3.5	4.1	3.2	0.34	$6.8\times10^{+0}$
4C 35.16A	9.4	7.4	7.0	5.5	0.65	2.9×10^{-1}
4C 53.16	23.4	18.3	–	–	1.83	3.6×10^{-2}
B2 0915+32	–	–	6.2	4.9	0.49	1.8×10^{-2}
NGC 4782	1.8	1.4	3.5	2.8	0.21	6.1×10^{-1}
B2 1322+36	–	–	3.3	2.6	0.26	2.6×10^{-2}
B2 1450+28	12.4	9.7	13.0	10.2	1.00	3.9×10^{-1}
B2 1525+29	9.9	7.8	6.9	5.4	0.66	7.5×10^{-1}
B2 1637+29	10.8	8.5	9.5	7.5	0.80	1.9×10^{-1}
3C 402N*	5.0	3.9	4.2	3.3	0.39	4.2×10^{-2}
3C 449	3.4	2.7	2.3	1.8	0.23	9.7×10^{-2}
B2 2236+35	6.7	5.3	8.3	6.5	0.59	4.5×10^{-3}
3C 465	4.9	3.8	5.4	4.2	0.40	$1.1\times10^{+0}$
4C 47.63	–	–	5.2	4.0	0.40	$\sim 1\times10^{-2}$

NOTES.—(*) IS parameter represents the addition due to the two companions detected around this galaxy.

The age estimates with the two different methods presented above agree to within a factor of less than 2. Therefore, the age of the collision (t_{age}) is defined as the average of the two age estimates, i.e., $t_{age} = 0.5 \times (t_{isophot} + t_{profile})$ in units of 10^8 yrs (see Table 7). On average, the age of the collision corresponds to 5.3×10^7 yrs, indicating the existence of a very recent, probably still ongoing, collision in these galaxies.

4.4. *Strength of the Collision*

The radial distance at which the light excess over a de Vaucouleurs law appears is a function only of the time elapsed since the gravitational encounter started while the absolute magnitude of the excess depends on the physical parameters of the collision (Aguilar & White 1986). Although a detailed analysis of the excess over the $r^{1/4}$ law as a function of the parameters of a collision is out of the scope of this paper, it is relevant here to stress the potential use of the information provided by these excesses (distance r_{excess} or radial dependence of the excess) in constraining the collision if it is combined with more detailed collisional models. However, a first parameterization of the strength of the collision can already be obtained by the parameter IS (interaction strength) defined as

$$\mathrm{IS} = t_{age}(M_c/M_R)d_{20}^{-3}\ , \qquad (9)$$

where t_{age} is the age of the collision in units of 10^8 yr as defined in § 4.4, M_c/M_R is the mass ratio of the galaxies involved in the collision (see Table 6), and d_{20}^{-3} is the pair's projected separation in units of 20 kpc. The results for the 21 FR I host colliding galaxies with reliable information are presented in Table 7. According to the IS parameter, which represents a measure of the tidal impulse suffered by the FR I host galaxy, the collisions are characterized by a median value IS = 0.19 but the values of the IS parameter cover a range of 4 orders of magnitude from a few times 10^{-3} to 10^{+1}.

If the working hypothesis of the collisionally induced activity in galaxies is true, it is difficult to understand why collisions covering four orders of magnitude in the interaction strength, produce such a well-defined type of FR I radio sources, covering basically one order of magnitude in the radio properties (Colina & Pérez-Fournon 1990b; de Juan & Colina 1995). It could be that collisions of galaxies is one of the triggers that ignites the chain of processes that occur in a galaxy resulting in the generation of a radio source. If this is correct, the values of the IS parameter would only indicate a certain threshold above which the chain of processes starts. In this context, the collision could be very efficient in concentrating the gas in the nuclear regions and after that trigger other mechanisms like the appearance of nuclear gas disks. Such disks as those recently discovered in NGC 4261 (Jaffe et al. 1993), M87 (Ford et al. 1994), 3C 449 (Capetti et al. 1994), and 3C 402N (de Juan & Colina 1995) could play a central role in the generation and fueling of the radio source long after the tidal impact generated during the close encounter is over. A further analysis and detailed study of these issues is clearly needed.

4.5. NGC 4782/4783: *Prototype of Colliding FR I Host Galaxy*

The system NGC 4782/NGC 4783 is the only FR I colliding pair in our sample for which both a detailed collisional model (Borne, Balcells, & Hoessel 1988), and simulation of the morphology of the associated 3C 278 radio source exists (Borne & Colina 1993).

As a check of the mass and age estimates presented in §§ 4.3 and 4.4 above, we compare our values with those obtained by Borne et al. (1988). These authors quoted a pair mass ratio of 0.7, and an age since pericenter passage of 2.5×10^7 yrs. Their results, based on a detailed collisional model completely independent from our methods, are in good agreement with our estimates of 0.44 for the mass ratio, and 2.1×10^7 yrs for the age of the collision, thus supporting the robustness of the collision characterization presented in § 4.

Detailed models of the radio jet morphology of 3C 278 (FR I source associated with NGC 4782) allowed Borne & Colina (1993) to conclude that the radio emission started some 5×10^7 yrs before the pericenter passage. Thus, if there is a gravitationally induced FR I radio source generation in the nuclei of ellipticals, this seems to happen very early in the history of the collision. In later phases, the tidal shocks generated in the deeply penetrating collision will affect the radio source by disrupting the radio morphology (Borne & Colina 1993) and, possibly as well, by changing the accretion rate into the black hole. The observed radio luminosity function of FR I dumbbell galaxies, flatter than that of single FR I host galaxies (Parma, Cameron & de Ruiter 1991), could be an observational signature of the differences in accretion rates.

5. COLLISION OF GALAXIES AND THE ONSET OF RADIO SOURCES: FR I VERSUS FR II HOST GALAXIES

The environment, stellar, and gas properties of the host galaxies associated with FR II radio sources has been studied extensively by Heckman and collaborators (Heckman et al. 1986; Baum et al. 1988; Baum & Heckman 1989a, b, c; Smith & Heckman 1989a, b). Powerful FR II host galaxies (labeled as SE in Smith & Heckman (1989a) are characterized by a $\mu_e - r_e$ relation given by

$$\text{FR II: } \mu_e(r \text{ mag arcsec}^{-2}) = 2.81(\pm0.30)\log r_e(\text{kpc}) + 19.59(\pm0.35)\ , \qquad (10)$$

which agrees, within the uncertainties, with the same relation obtained for FR I host galaxies (see § 4).

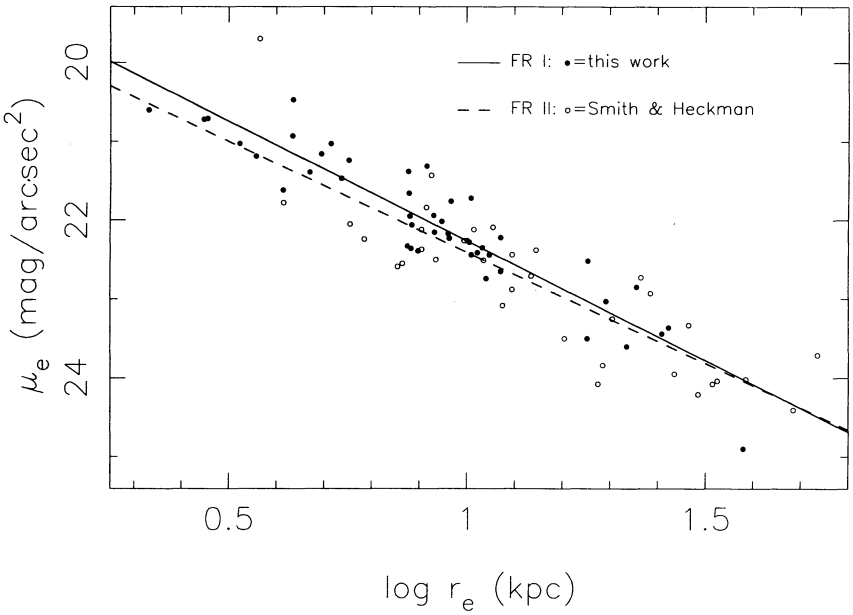

FIG. 5.—$\mu_e - r_e$ relation for FR I and FR II host galaxies (see § 5 for details)

However, FR II host galaxies tend to be produced by ellipticals that have a larger effective radius and a fainter effective magnitude than FR I host galaxies (Fig. 5). On the average, FR I host galaxies are characterized by an effective surface brightness and radius of 22.04 ± 0.90 mag arcsec^{-2} and 10.4 ± 7.3 kpc, respectively; for FR II host galaxies these values are 22.82 ± 0.98 mag arcsec^{-2} and 17.6 ± 12.7 kpc, respectively. This difference, together with the already mentioned differences in the environment (see § 4 and references), and perhaps in the ellipticity distribution (see § 4.1.2), indicate that FR I and FR II host galaxies are intrinsically different types of ellipticals, in general.

Moreover, FR II host galaxies show evidence of morphological distortions in the form of long tidal tails, shells and dust lanes across the galaxy (Heckman et al. 1986). Also, the warm optical emission line gas is distributed with irregular morphologies over very extended regions up to 100 kpc in size and with a medium size of 10 kpc (Baum et al. 1988). The amount of ionized gas ($M \sim 10^8$–10^9 $M_\odot$) derived from the Hα luminosities (Baum & Heckman 1989c) indicates that FR II host galaxies are systems rich in gas. All these characteristics are interpreted in terms of the residuals of past collisions or mergers between a bright elliptical, i.e., the host of the FR II source, and a gas-rich system, i.e., a spiral.

On the other hand, FR I radio sources are associated with bright ellipticals that are, in many cases, colliding with a small elliptical and with no evidence for larger amounts of warm Hα emitting gas than in nonradio ellipticals (de Juan 1994).

It can be concluded that while a large fraction of FR II radio sources are found in bright ellipticals with evidence of a past collision or merger with a spiral, many FR I sources are found in bright ellipticals involved in a recent close collision with another elliptical, a factor of three smaller in size.

Collisions of galaxies are by no means the unique mechanism used by nature to channel gas into the inner most regions of a galaxy to produce radio sources. Additional types of mechanisms which involve nuclear disks of gas and dust like those found in NGC 4621 (Jaffe et al. 1993), M 87 (Ford et al. 1994), 3C 449 (Capetti et al. 1994), and 3C 402N (de Juan, Colina, & Golombek 1995) can also be very efficient in generating and sustaining transient radio activity in galaxies (see also discussion in § 4.4).

6. CONCLUSIONS

The first detailed quantitative study on the characterization of FR I host galaxies based on a detailed two dimensional morphological analysis of a large sample of FR I host galaxies has been presented. The conclusions of this study can be summarized as follows:

1. A large fraction of the FR I host galaxies in the sample show in their stellar distribution clear evidence of at least one (86%), two (60%), or three (47%) morphological distortions not frequently observed in isolated ellipticals. These distortions, considered as signatures of recent collisions, include: (1) isophote twists larger than 15°, (2) isophote displacements larger than 3.5%, (3) light excess over a $r^{1/4}$ law larger than 0.1 mag arcsec^{-2} at radii beyond r_e, and (4) the presence of companion ellipticals at a distance of less than 50 kpc.

2. Based on the $\mu_e - r_e$ relation and on the ellipticity distribution, FR I host galaxies are bright ellipticals and, perhaps, rounder than the average elliptical.

3. The collisions involving FR I host galaxies are characterized (in the median) by (1) a mass ratio (companion to FR I host galaxy) of 0.2, (2) a projected separation of 23 kpc, (3) a relative velocity of 492 km s^{-1}, (4) an age of 4.0×10^7 years, and (5) an interaction strength parameters IS = 0.19.

4. On average, FR I host galaxies have a brighter effective brightness, and a smaller effective radius than FR II host galaxies.

5. The causal connection between collision of galaxies and onset of nuclear activity in galaxies, well established for luminous *IRAS* galaxies, quasars, and FR II radio sources, can be extended to FR I radio sources.

In a broader picture, the study presented in this paper, adds strong support to the idea that collisions/mergers involving different types of galaxies are able to generate a different kind

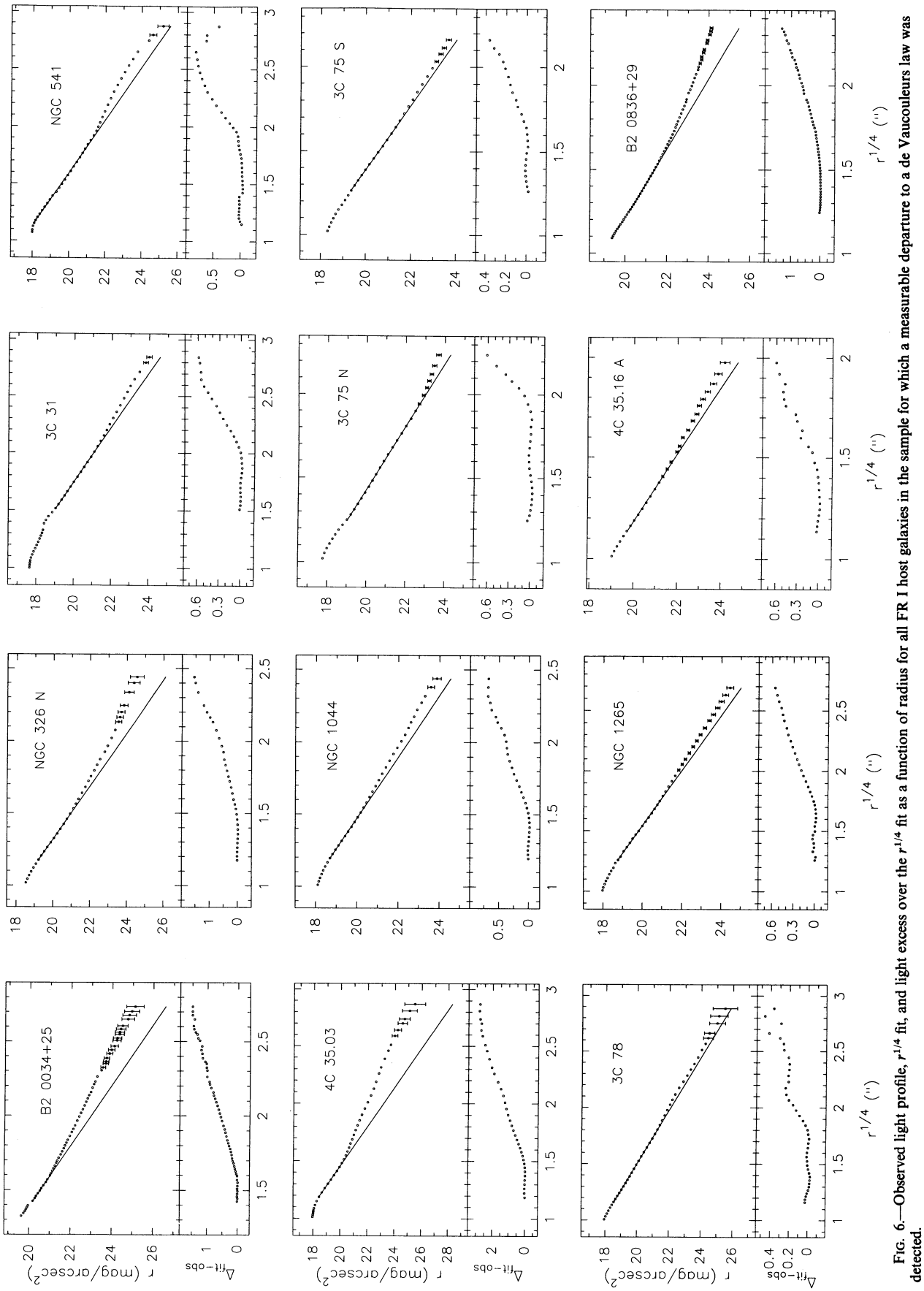

FIG. 6.—Observed light profile, $r^{1/4}$ fit, and light excess over the $r^{1/4}$ fit as a function of radius for all FR I host galaxies in the sample for which a measurable departure to a de Vaucouleurs law was detected.

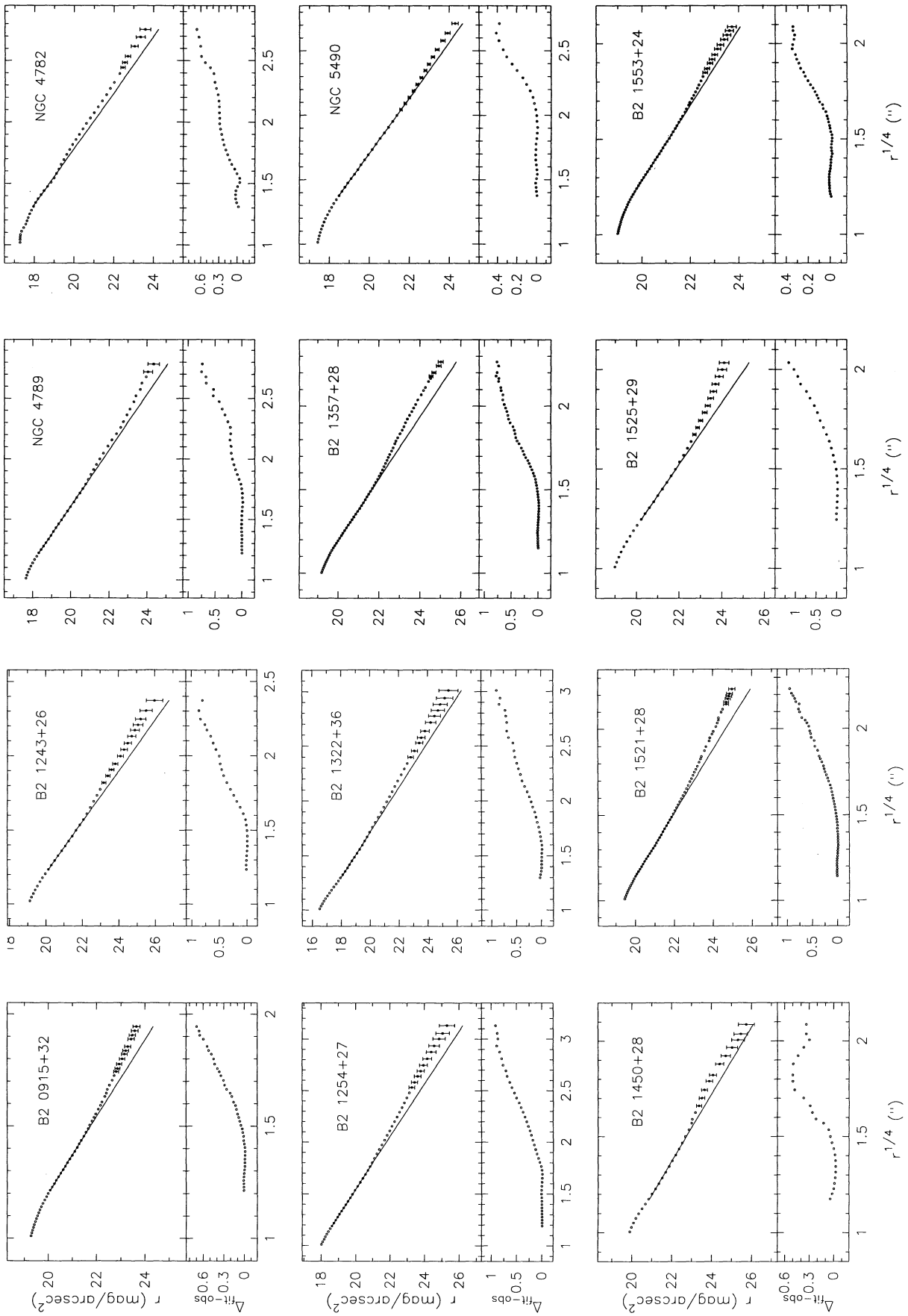

FIG. 6—*Continued*

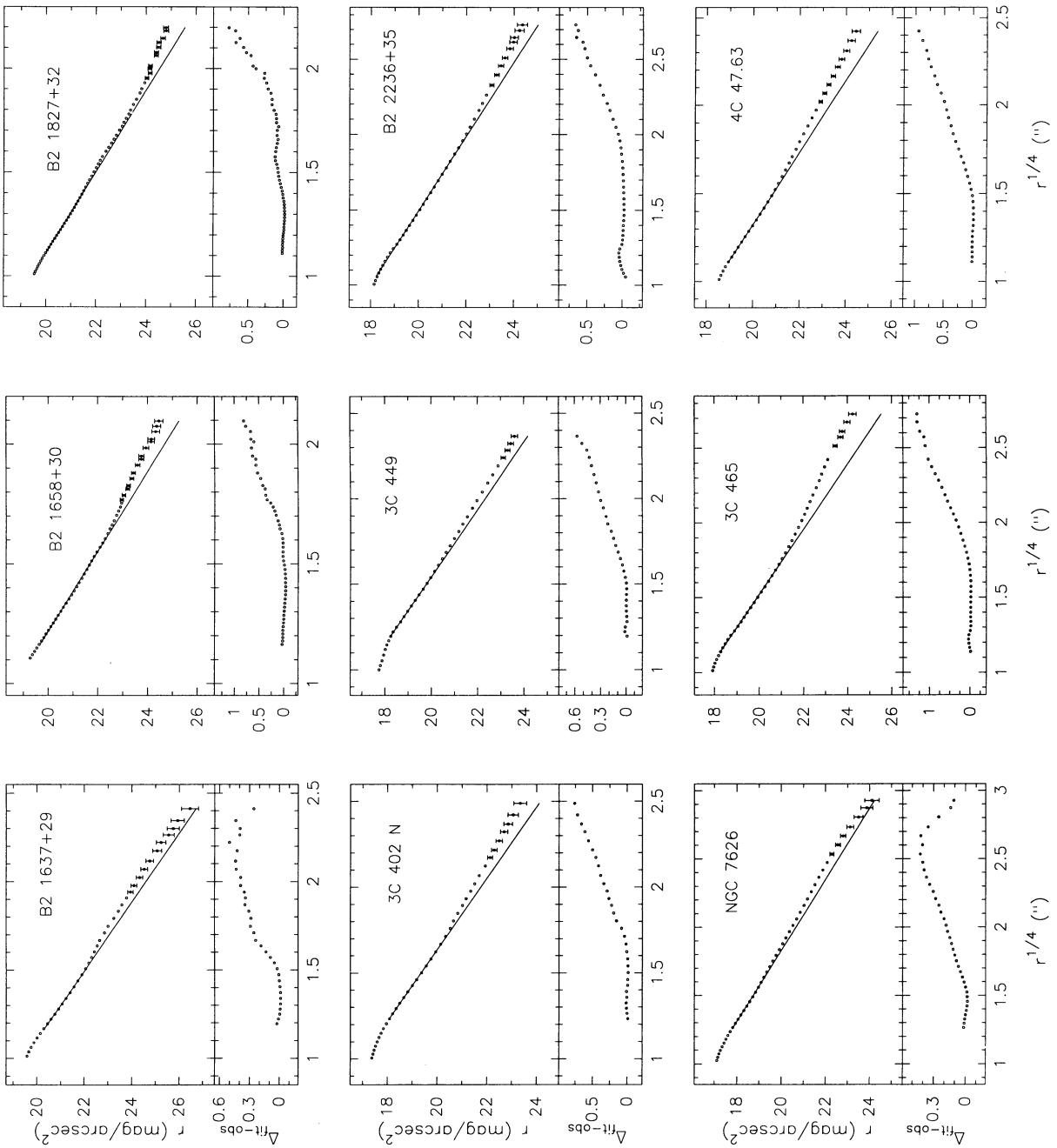

FIG. 6—*Continued*

of nuclear and/or circumnuclear activity: collisions/mergers between spirals produce luminous starburst infrared galaxies, collisions/mergers between a bright elliptical and a spiral generate luminous FR II radio sources, and collisions involving two ellipticals create low luminosity FR I radio sources.

We wish to thank J. I. González-Serrano for allowing us to analyze unpublished images and data from his sample of radio galaxies. Thanks also to L. Binette, and K. D. Borne for their detailed comments and suggestions on an early version of this paper. Lourdes de Juan benefited from a short-term stay at the STScI through its Visitor Program. This work has been partially supported by the Spanish Council for Research and Technology under grant PB90-0182.

APPENDIX

A large fraction of the galaxies in the sample show light profiles that depart from a $r^{1/4}$ law fitted to the inner region (see § 3.3 and Table 3 for details). Figures in this appendix (Fig. 6) represent the light profile in r-magnitudes for each galaxy showing this behavior, the $r^{1/4}$ fitted law, and the excess over this law (the latter labeled "$\Delta_{\text{fit-obs}}$" and measured in mag arcsec^{-2}).

REFERENCES

Aguilar, L. A., & White, S. D. M. 1986, ApJ, 307, 97
Baum, S. A., & Heckman, T. 1989a, ApJ, 336, 681
———. 1989b, ApJ, 336, 702
———. 1989c, ApJ, 338, 48
Baum, S. A., Heckman, T., Bridle, A., van Breugel, W. H. M., & Miley, G. K. 1988, ApJS, 68, 643
Benacchio, L., & Galletta, G. 1980, MNRAS, 193, 885
Bender, R., Döbereiner, S., & Möllenhoff, C. 1987, A&AS, 74, 385
Borne, K. D. 1984, ApJ, 287, 503
Borne, K. D., Balcells, M., & Hoessel, J. G. 1988, ApJ, 333, 567
Borne, K. D., & Colina, L. 1993, ApJ, 416, 157
Bridle, A. H., & Perley, R. A. 1984, ARA&A, 22, 319
Capetti, A., Macchetto, F. D., Sparks, W. B., & Miley, G. K. 1994, A&A, 289, 61
Colina, L., & Pérez-Fournon, I. 1990a, ApJS, 72, 41
———. 1990b, ApJ, 346, 45
de Juan, L. 1994, Ph.D. thesis, Autonoma Univ. Madrid
de Juan, L., Colina, L., & Golombek, D. 1995, A&A, submitted
de Juan, L., Colina, L., & Pérez-Fournon, I. 1994, ApJS, 91, 507
de Ruiter, H. R., Parma, P., Fanti, R., & Ekers, R. D. 1988, ApJ, 329, 225
Disney, M. J., Sparks, W. B., & Wall, J. V. 1984, MNRAS, 206, 899
Ford, H. C., et al. 1994, ApJ, 435, L27
González-Serrano, J. I., Carballo, R., & Pérez-Fournon, I. 1993, AJ, 105, 1710
Heckman, T. M. 1991, in IAU Colloq. 124, Paired and Interacting Galaxies
Heckman, T. M., Carty, J. J., & Bothun, G. D. 1985, ApJ, 288, 122
Heckman, T. M., Smith, E. P., Baum, S. A., van Breugel, W., Miley, G. K., Illingworth, G. D., Bothun, G. D., & Balick, B. 1986, ApJ, 311, 526
Hoessel, J. G., Oegerle, W. R., & Schneider, D. P. 1987, AJ, 94, 1111
Hutchings, J. B., & Neff, S. G. 1992, AJ, 104, 1
Jaffe, W., Ford, H. C., Ferrarese, L., van den Bosch, F., & O'Connell, R. W. 1993, Nature, 364, 213
Kent, S. M. 1985, PASP, 97, 165
Kormendy, J. 1977, ApJ, 218, 333
Kormendy, J. 1982, in Morphology and Dynamics of Galaxies, 12th Advanced Course of the Swiss Society of Astronomy and Astrophysics, ed. L. Martinet & M. Mayor (Sauverny: Geneva Obs.), 113
Kormendy, J., & Djorgovski, S. 1989, ARA&A, 27, 235
Lauer, T. R. 1985, MNRAS, 216, 429
———. 1988, ApJ, 325, 49
Lilly, S. J., & Prestage, R. M. 1987, MNRAS, 225, 531
Longair, M. S., & Seldner, M. 1979, MNRAS, 189, 433
Melnick, J., & Mirabel, F. 1990, A&A, 231, L19
Mihalas, D., & Binney, J. 1981, Galactic Astronomy. Structure and Kinematics (San Francisco: Freeman)
Parma, P., Cameron, R. A., & de Ruiter, H. R. 1991, AJ, 102, 1960
Sanders, D. B., Soifer, B. T., Elias, J. H., Madore, B. F., Matthews, K., Neugebauer, G., & Scoville, N. Z. 1988, ApJ, 325, 74
Schombert, J. M. 1986, ApJS, 60, 603
———. 1988, ApJ, 328, 475
Smith, E. P., & Heckman, T. M. 1989a, ApJ, 341, 658
———. 1989b, ApJS, 69, 365
Soares, D. S. L. 1989, Ph.D. thesis, Univ. Groningen
Sparks, W. B., Wall, J. V., Jorden, P. R., Thorne, D. J., & van Breda, I. 1991, ApJS, 76, 471
Valentijn, E. A., & Casertano, S. 1988, A&A, 206, 27
Wirth, A., Smarr, L., & Gallagher, J. S. 1982, AJ, 87, 602